Supplementary information: BSE images of analyzed crystals and SIMS analysis craters

Numbers refer to the corresponding analyses as indicated in the SIMS data table (red = excluded from weighted mean calculations). Frames and numbers in blue indicate crystals selected for ID-TIMS analysis.

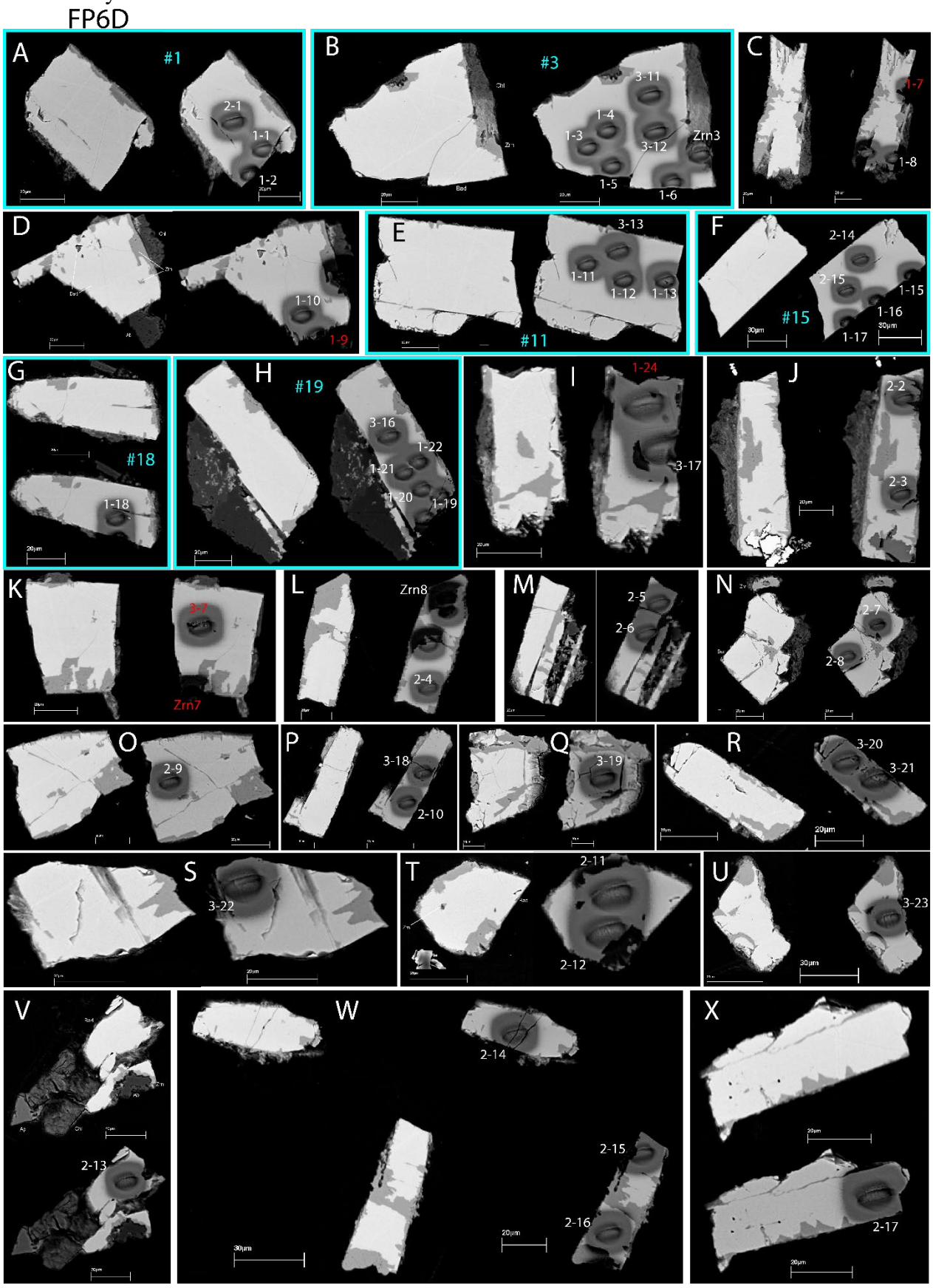

Figure S1. BSE images of analyzed baddeleyite and zircon crystals and SIMS analysis craters of sample FP6D (grain mount).

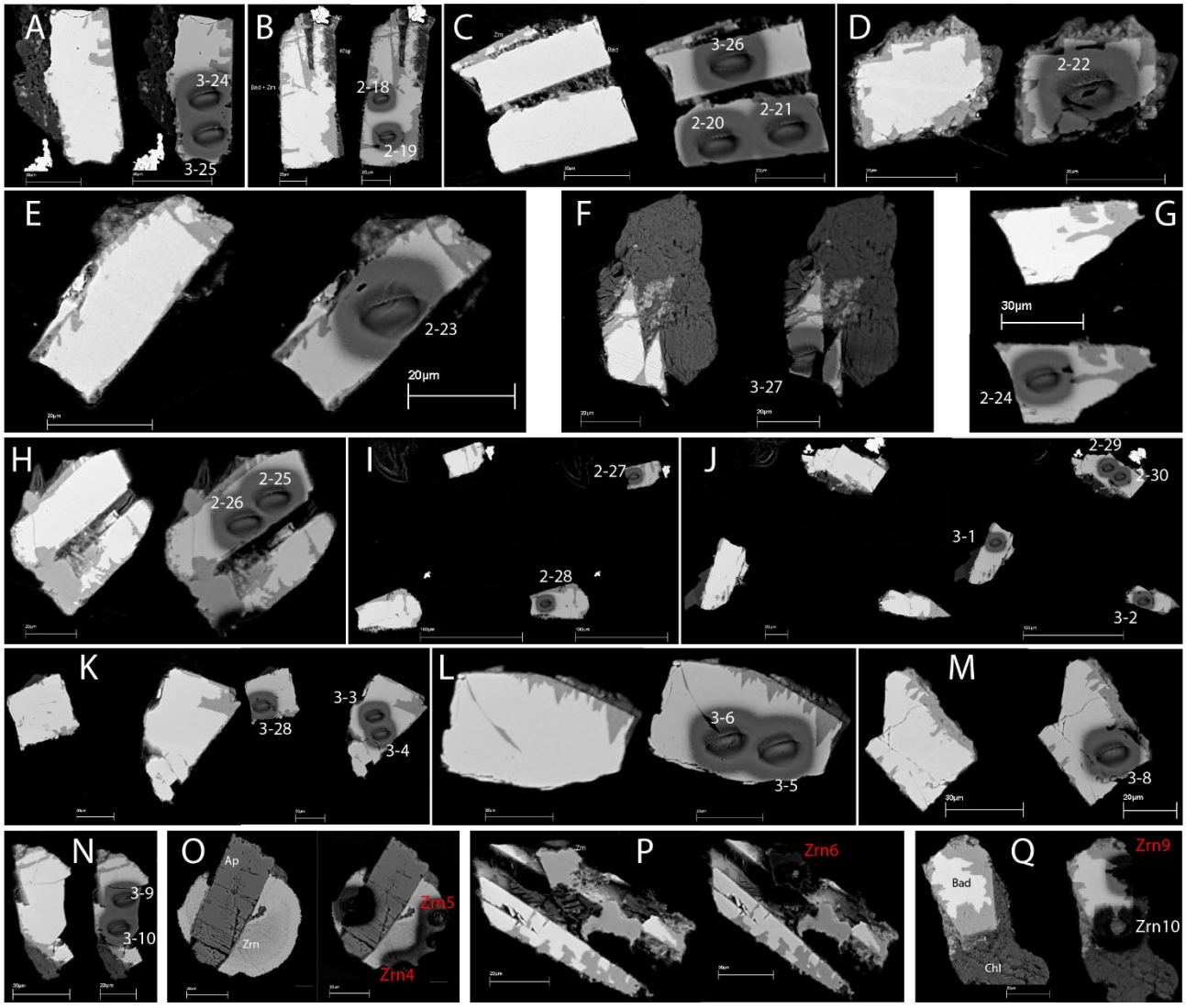

Figure S2. BSE images of analyzed baddeleyite and zircon crystals and SIMS analysis craters of sample FP6D (grain mount), continued.

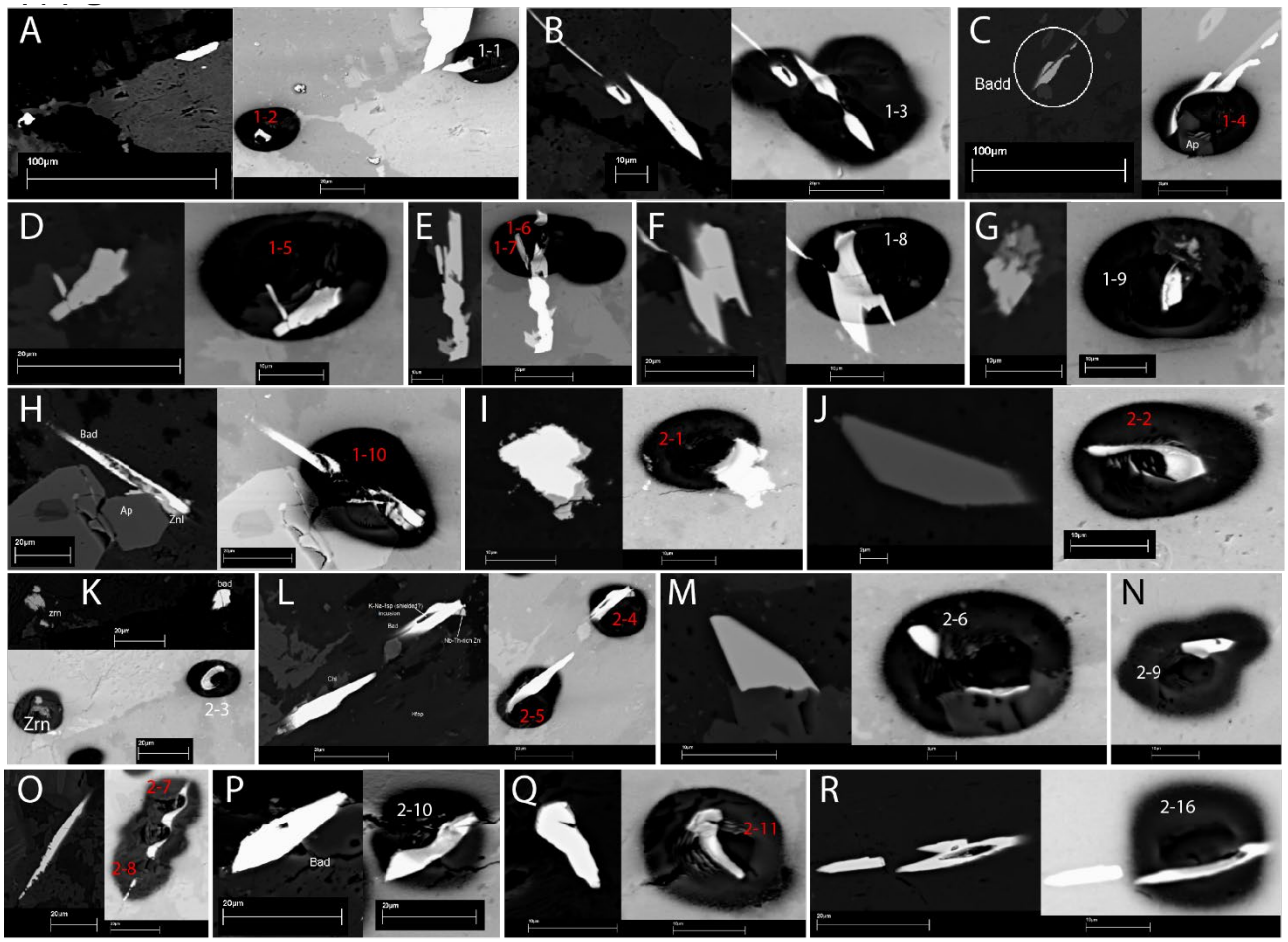

Fig. S3. BSE images of analyzed crystals and SIMS analysis craters of sample FP7G (in situ).

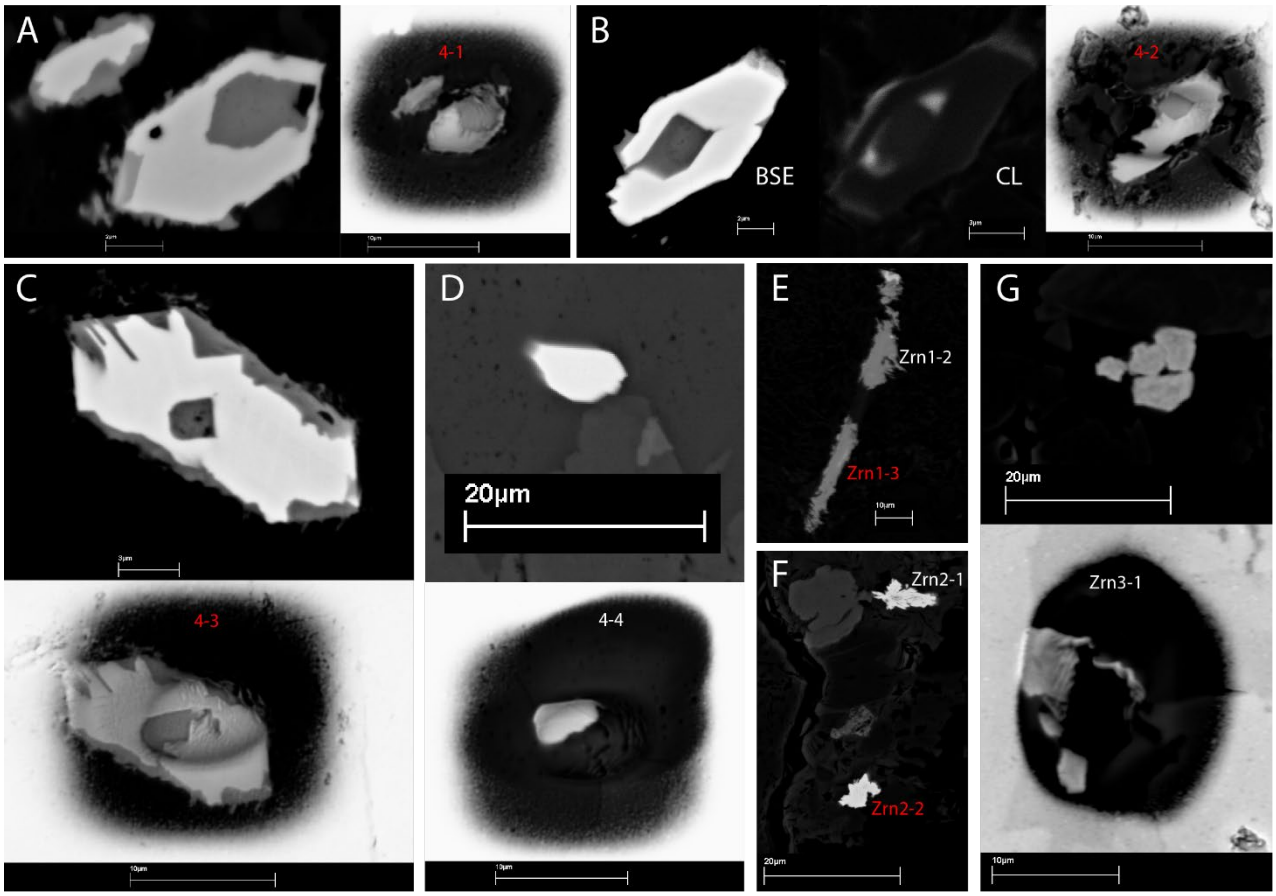

Figure S4. BSE images of analyzed baddeleyite crystals with zircon inclusions and SIMS analysis craters of sample FP12A (in situ).

FP12A

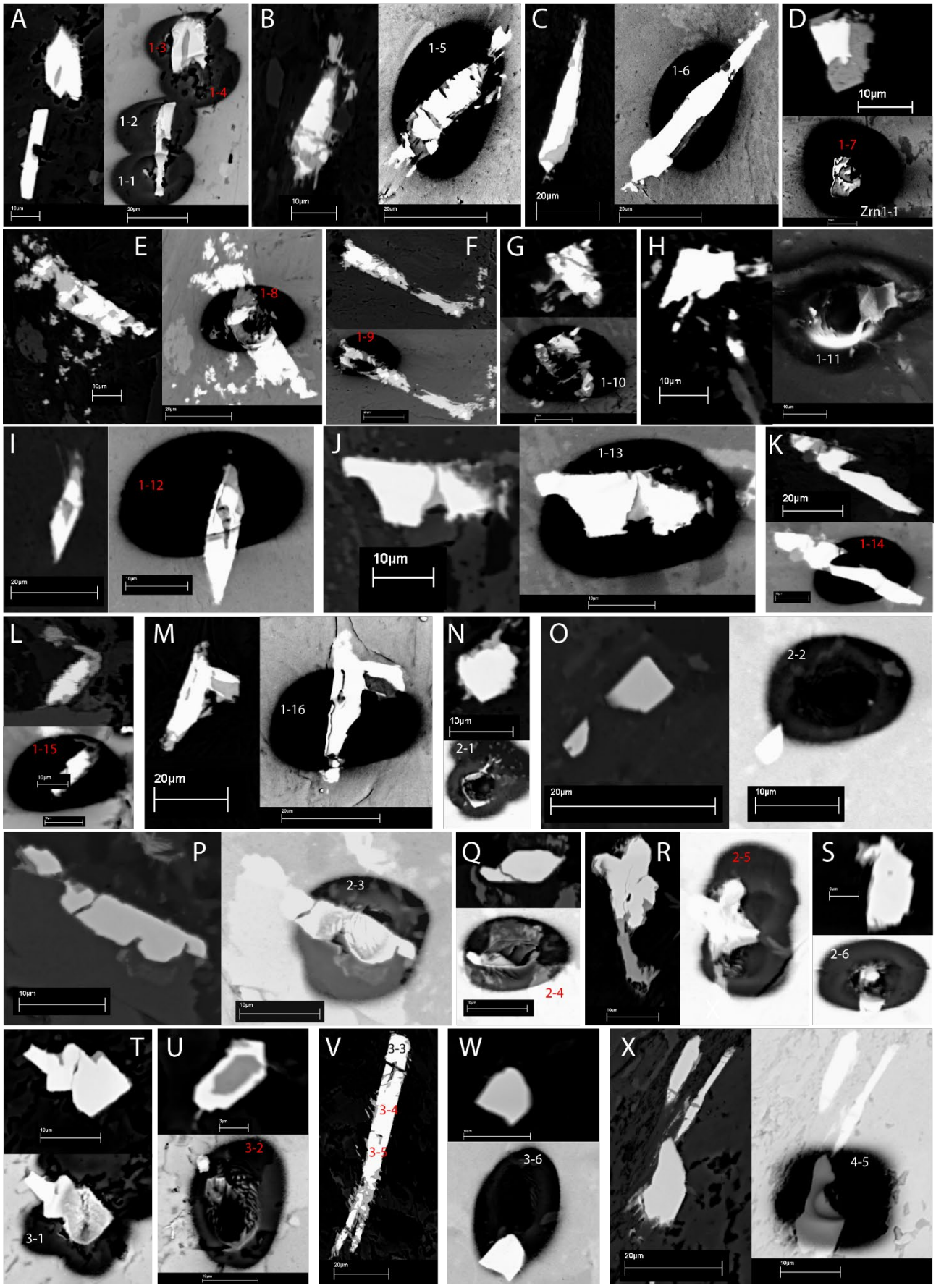

Figure S5. BSE images of analyzed crystals and SIMS analysis craters of sample FP12A (in situ). Numbers refer to the corresponding analyses as indicated in the data table.

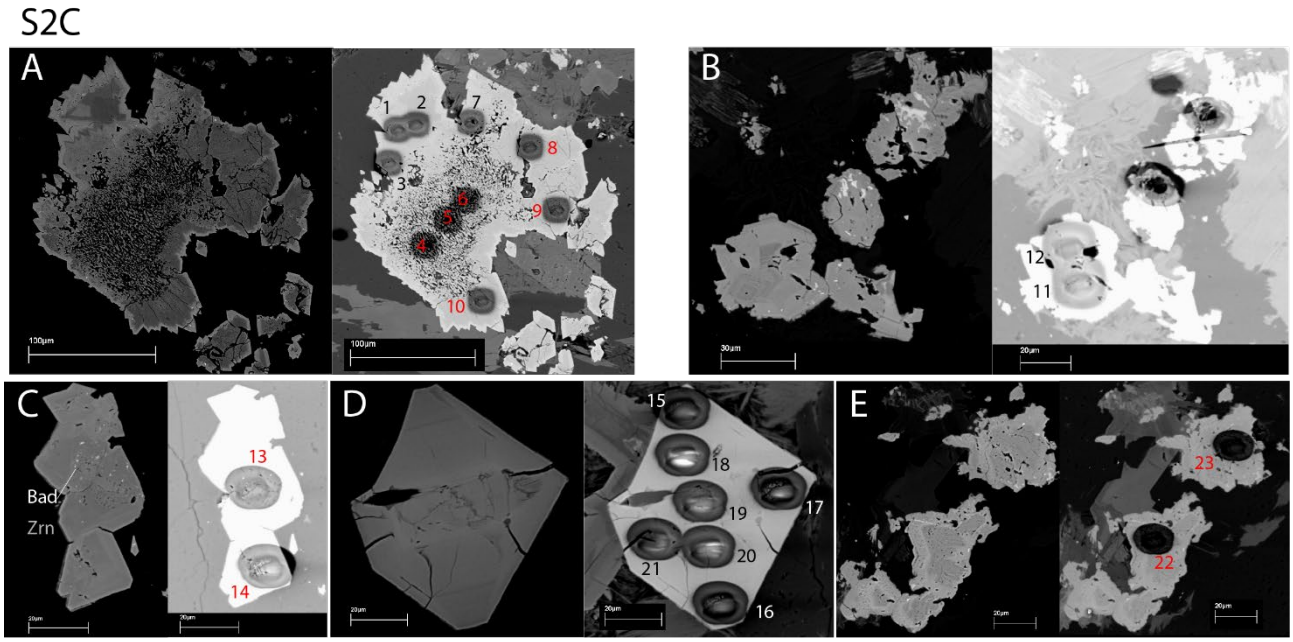

Figure S6. BSE images of analyzed crystals and SIMS analysis craters of sample S2C (in situ).

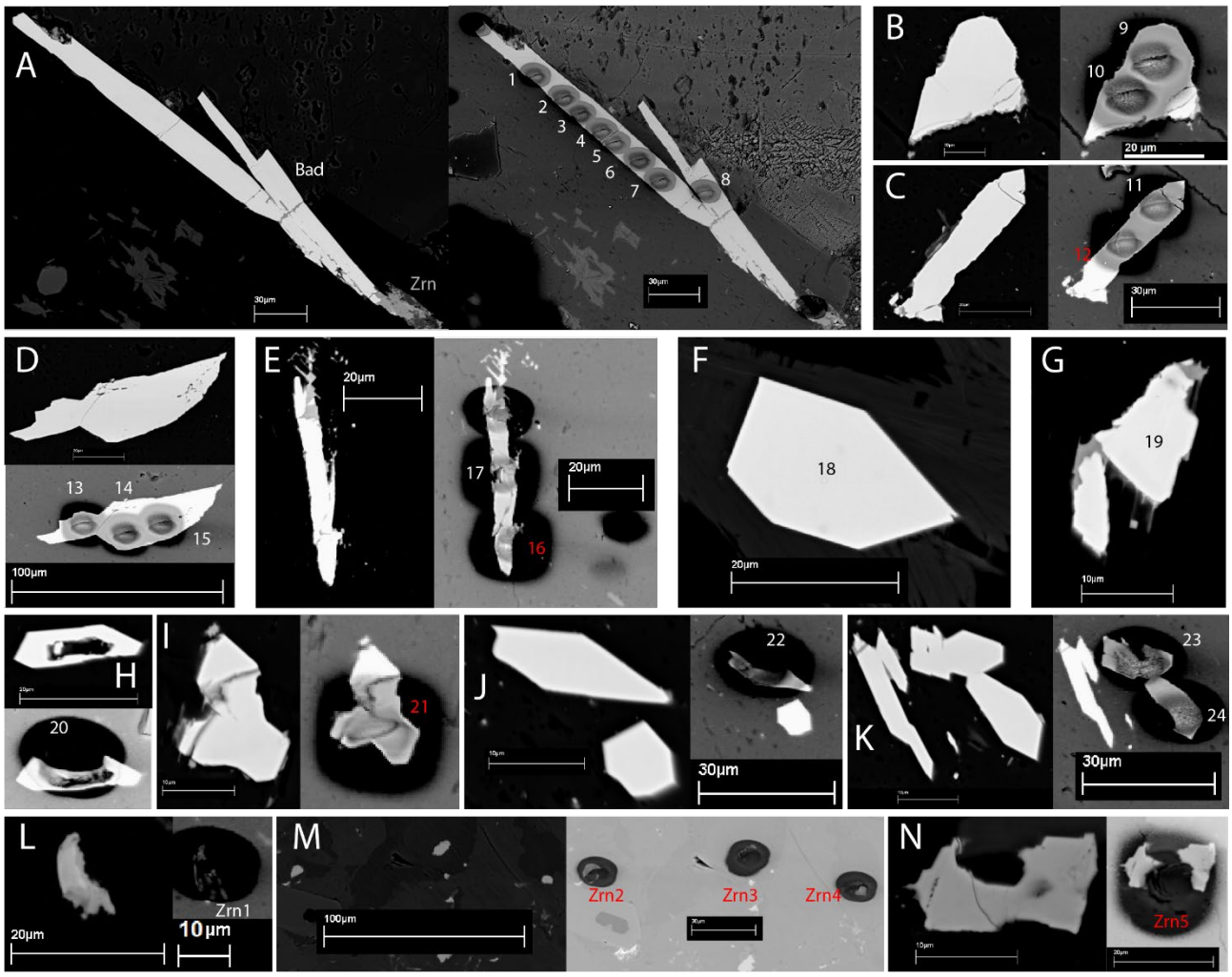

Figure S7. BSE images of analyzed crystals and SIMS analysis craters of sample S2E (in situ).

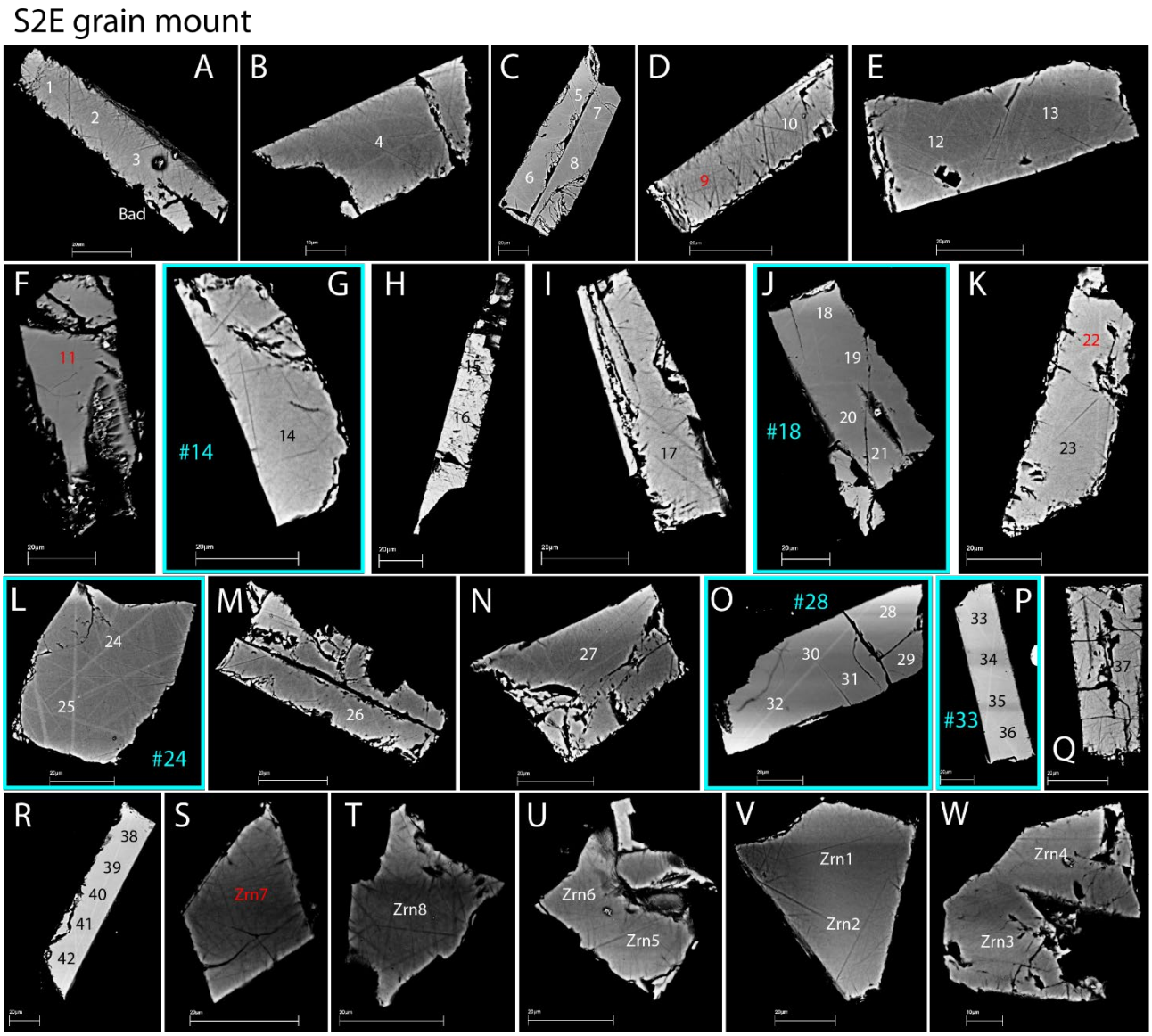

Figure S8. BSE images of analyzed crystals and SIMS analysis craters of the grain mount of sample S2E.

Details of SIMS and ID-TIMS U-Pb preparation and analytical conditions

For preparing in situ mounts, baddeleyite-bearing parts of petrographic thin section were cut using a diamond saw, and mounted in a 25.4 mm epoxy disk along with pre-polished epoxy blocks of reference baddeleyite and/or zircon. Grain mounts were made when crystals detected in thin section were large enough for mineral separation (>50 µm). In this case, the rock was crushed and sieved to <200 µm. Usage of the electromagnetic Frantz separator at 1.5–2.0 A and 5–15° tilt was found inefficient, and hence abandoned. Instead, baddeleyite was concentrated via hydraulic separation in a water-filled bowl, followed by hand picking under a binocular microscope. Separated crystals were then embedded in epoxy along with reference baddeleyite and/or zircon, and sectioned using SiC paper (4000 grit) and diamond suspension (1 µm, ¼ µm).

Automated mass calibration for SIMS analysis was employed, with shifts for Pb peaks referenced to that for Zr_2O, and the Th species (Th and ThO) against U and UO_2, respectively. For analyses of reference materials and grain mount sessions, a chain of spots was run automatically, employing automated pre-sputtering and beam centering. When unknowns of in situ analyses were analyzed, automated analysis chains were not applicable, so the Z position of the sample stage had to be adjusted manually prior to each analysis, compensating slight differences in sample height. Beam centering and spot finding were executed in the same step by using the $^{180}Hf^{16}O$ secondary ion image. The $^{206}Pb/^{238}U$ age and U concentrations of the reference materials were used to calculate those of the samples. Baddeleyite, zircon and zirconolite were analyzed in multiple sessions between 10/19/2017 and 07/20/2018. All SIMS data have been evaluated using the ZIPS software (version 3.1.1).

For ID-TIMS data from S2E and FP6D, baddeleyite grains were plucked from the SIMS mount, spiked with $^{205}Pb/^{233}U/^{235}U$ tracer (ET535) and dissolved in HCl acid in teflon microcapsules. ID-TIMS measurements used single Daly-photomultiplier mode on a Micromass Sector 54 thermal ionization mass spectrometer at the University of Wyoming. Mass discrimination for Pb was 0.200 ± 0.10 %/amu for Daly analyses based on replicate analyses of NIST SRM 981. U fractionation was determined internally during each run. Measured procedural blanks averaged 0.8 pg Pb. U blanks were consistently less than 0.1 pg. Isotopic composition of the Pb blank was measured as 18.5268 ± 0.45, 15.6046 ± 0.41, and 38.0332 ± 0.73 for $^{206}Pb/^{204}Pb$, $^{207}Pb/^{204}Pb$ and $^{208}Pb/^{204}Pb$, respectively. The sample weight was estimated from grain dimensions assuming a density of 6.02 g/cm^3; U and Pb concentrations are based on these estimates. Picograms (pg) sample and common Pb are measured directly from isotope dilution measurements.

Geochemistry - analytical conditions

All geochemical analyses were performed by geochemical laboratories of the GFZ Potsdam. Concentrations of major elements (reported in oxide wt. % with Fe as Fe_2O_3) and trace elements (Rb, Sr, Ba, Y, Zr, Nb, Zn, Cu, Ni and V) were determined by X-ray fluorescence spectrometry. Powdered samples were prepared as fused discs of Li tetraborate-metaborate (FLUXANA FX-× 65, sample-to-flux ratio 1:6) and analyzed with a PANalytical AXIOS Advanced spectrometer employing a Rh X-ray tube. H_2O and CO_2 concentrations were determined by pyrolysis with a EURO EA Element Analyzer.

Following acid dissolution of the powdered samples, further trace elements were analyzed with an ELEMENT 2XR high-resolution sector field mass spectrometer (HR-ICP-MS) using inductively coupled plasma as an ion source. The following isotopes were used for analysis: ^{7}Li, ^{9}Be, ^{45}Sc, ^{59}Co, ^{63}Cu, ^{75}As, ^{98}Mo, ^{114}Cd, ^{118}Sn, ^{121}Sb, ^{133}Cs, ^{178}Hf, ^{205}Tl, ^{208}Pb, ^{209}Bi, ^{232}Th, ^{238}U. The values reported are the average of duplicate measurements from the same solution.

The rare-earth elements were analyzed by Inductively Coupled Plasma Optical Emission Spectrometry (ICP-OES) after a lithium metaborate-sodium perborate dissolution followed by the column purification technique. With an Agilent 5110

ICP-OES, the isotopes ^{139}La, ^{140}Ce, ^{141}Pr, ^{146}Nd, ^{149}Sm, ^{151}Eu, ^{157}Gd, ^{159}Tb, ^{163}Dy, ^{165}Ho, ^{167}Er, ^{169}Tm, ^{172}Yb, and ^{175}Lu were analyzed in high-resolution mode.

SIMS results for sample S2C (zircon)

Zircon dates from S2C are largely in the similar range as those for S2E baddeleyite, but some analyses are up to 50% younger (Fig. S9; Table S4). Most analyses show high common Pb, especially those with the youngest ages. Baddeleyite inclusions in zircon were too small to analyze.

Geochemistry – results

Results for major and trace elements (Table S7; Fig. S10-S12) are in good agreement with the data of Greenough (1984), except the rare earth elements, which he analyzed by X-ray fluorescence.

Supplementary references:

Sun, S.-s. and McDonough, W. F.: Chemical and isotopic systematics of oceanic basalts: implications for mantle composition and processes. Geological Society, London, Special Publications, 42(1), 313–345, 1989.

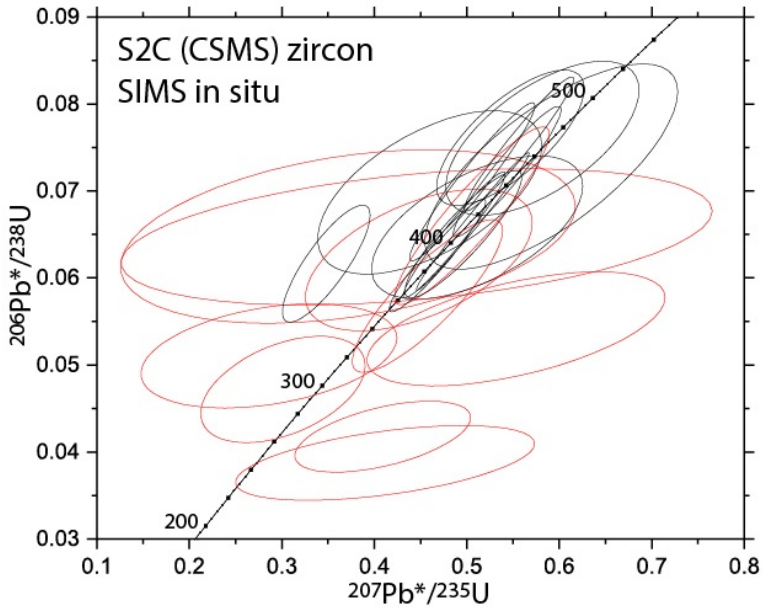

Figure S9. U-Pb results of S2C (1σ error ellipses). Analyses in red are those with the highest proportion of common Pb.

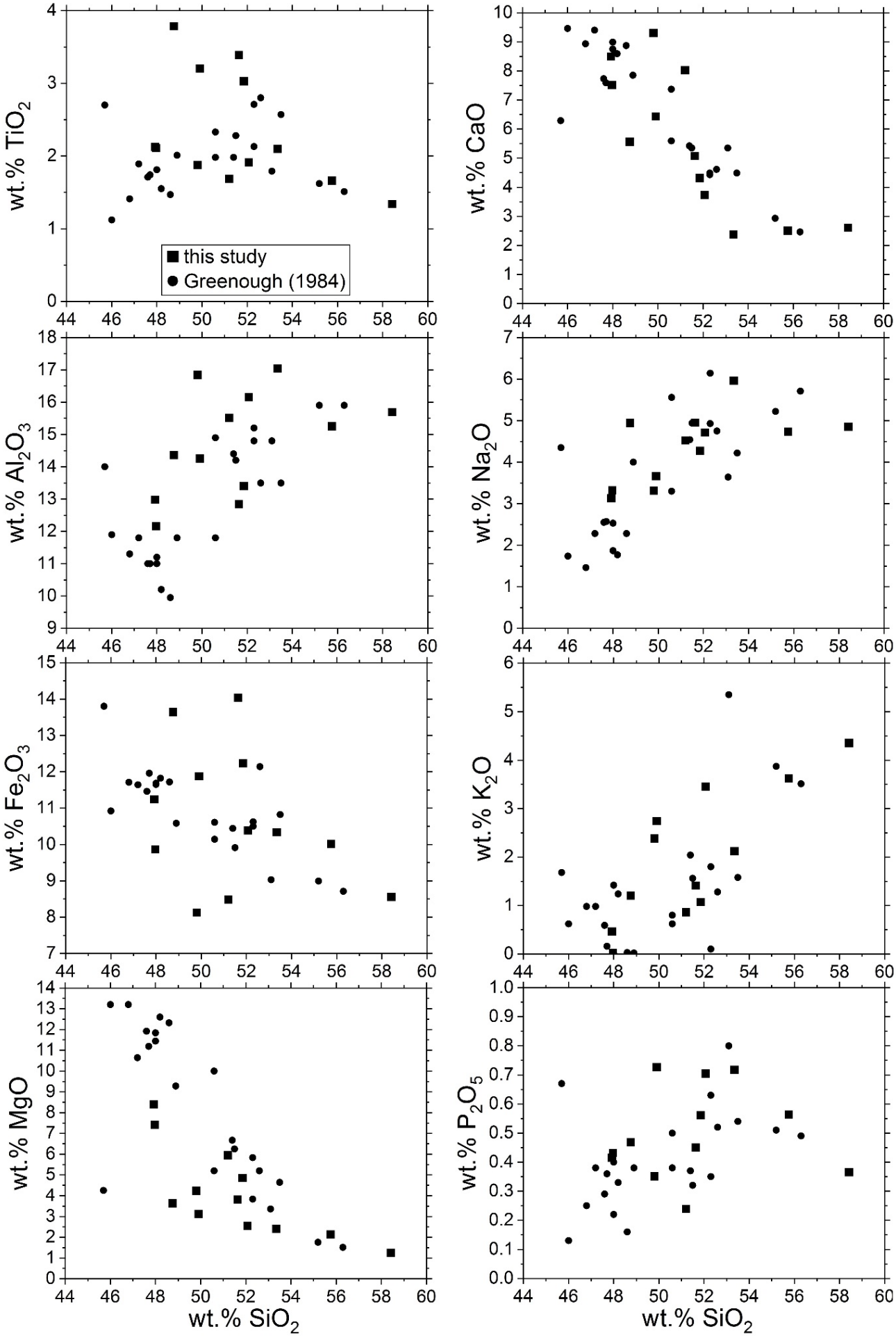

Figure S10. Major element contents of rocks from the Spread Eagle Intrusive Complex.

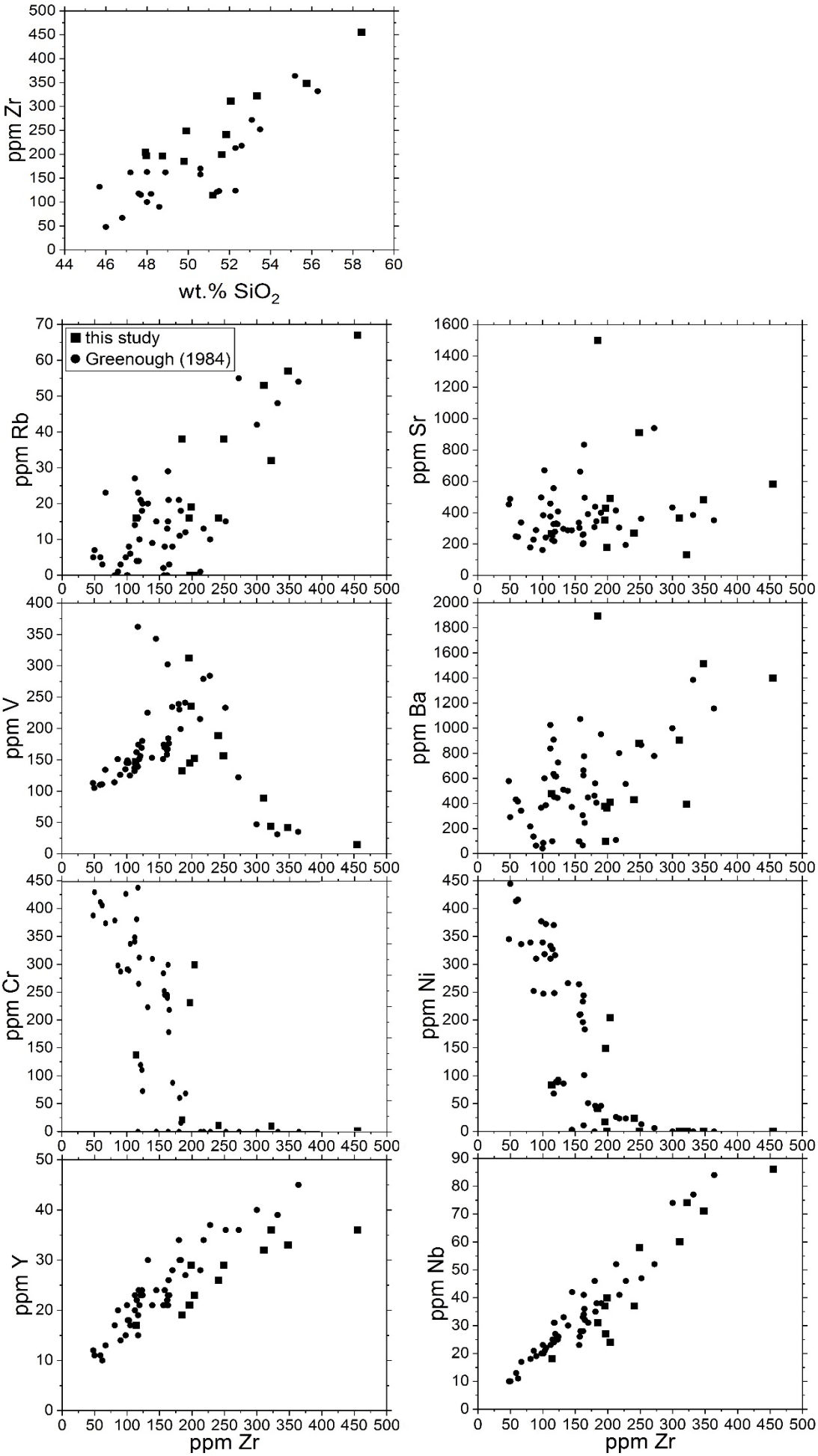

Figure S11. Trace element contents of rocks from the Spread Eagle Intrusive Complex.

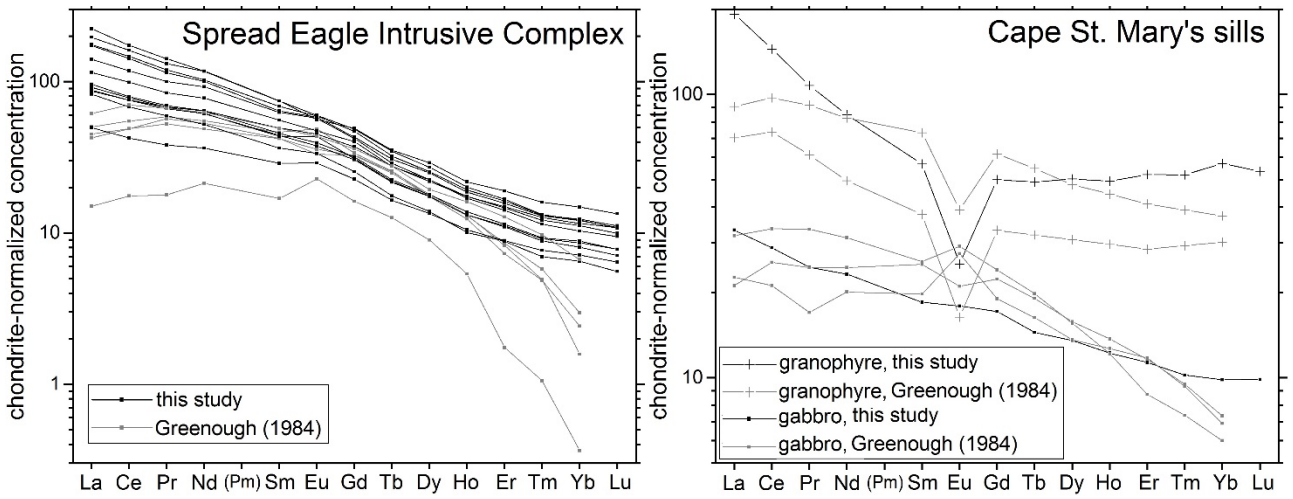

Figure S12. Rare earth element contents of rocks from the Spread Eagle Intrusive Complex and Cape St. Mary's sills, normalized to chondritic values after Sun and McDonough (1989). Note that the analyses of Greenough (1984) were done by X-ray fluorescence spectrometry, whereas ICP-OES was employed in our study.